International Journal of Mass Spectrometry 301 (2011) 166–173

Contents lists available at ScienceDirect

International Journal of Mass Spectrometry

journal homepage: www.elsevier.com/locate/ijms

# Increased ion transmission in IMS: A high resolution, periodic-focusing DC ion guide ion mobility spectrometer

Ryan C. Blase[a], Joshua A. Silveira[a], Kent J. Gillig[b], Chaminda M. Gamage[a], David H. Russell[a,*]

[a] Department of Chemistry, Texas A&M University, College Station, TX 77842-3012, USA
[b] Academia Sinica, 128 Academia Road, Section 2, Nankang, Taipei, 115, Taiwan

ARTICLE INFO

*Article history:*
Received 19 April 2010
Received in revised form 18 August 2010
Accepted 18 August 2010
Available online 26 August 2010

*Keywords:*
Periodic-focusing
Ion mobility spectrometry
Mass spectrometry
Ion mobility resolution
Ion transmission

ABSTRACT

The resolution of ion mobility spectrometry (IMS) is of paramount importance for both post-ionization separations and structural characterization of ions that have similar ion-neutral collision cross sections; however, the instrumental features that lead to increased resolution also decrease ion transmission through the drift cell. The periodic-focusing DC ion guide (PDC IG) drift cell provides increased ion transmission with minimal loss in resolution.

In earlier work we showed that the electrode geometry (inner diameter, thickness, and spacing) strongly affects ion focusing and ion transmission. Here, we critically evaluate the effect of the electrode geometry of a PDC IG drift cell on both ion transmission and resolution. In this study we examine two drift cells that differ in length (63 and 125 cm) and electrode configuration. We also examine the effects of applied voltage and pressure in an attempt to maximize both resolution and ion transmission. Experimental data obtained with fullerene and model peptide ions are compared with calculated ion trajectories using SIMION 8.0 simulations.

Published by Elsevier B.V.

## 1. Introduction

Ion mobility spectrometry (IMS) has significantly expanded our capabilities for mass spectrometry based studies for both small molecules [1,2] and macromolecules [3,4]. The orthogonal, two-dimensional separation of IM-MS offers increased peak capacity [5,6] as well as the ability to distinguish different chemical families [7,8]. Mass spectrometry provides accurate measurement of mass-to-charge ($m/z$) ratios, whereas IMS separates gas-phase ions on the basis of ion-neutral collision cross section [9,10]. The experimentally determined collision cross section can then be compared to collision cross sections determined by molecular dynamics (MD) simulations [11], and this information can be complementary to data obtained from tandem mass spectrometry and/or H/D exchange experiments for ion structure elucidation [7,12].

Resolution is the most significant limitation of IMS for interrogation of complex biological mixtures whether for post-ionization separation, analytical applications, and/or structural characterization of ions which have similar ion-neutral collision cross sections [7,13]. Diffusion limited resolution is defined by Eq. (1) [14,15]

$$R_d = \left(\frac{ELez}{16k_bT\ln 2}\right)^{1/2} \quad (1)$$

where $E$ is the electric field, $L$ is drift length, $z$ and $e$ are the numbers of charges and elementary charge, $k_b$ is the Boltzmann constant, and $T$ is drift gas temperature. Several approaches designed for increasing resolution have been described, and each of these approaches are aimed at one of the fundamental resolution-determining elements given by Eq. (1), *viz.* drift cell length ($L$) [16–22], electric field strength ($E$) [23–27], and temperature of the drift gas ($T$) [28–30]. However, the investigation of applied voltage, or electric field strength, on resolution has been limited owing to the use of drift cell lengths less than 30 cm. Increasing the drift cell length permits higher voltages to be applied prior to reaching electrical breakdown through the drift gas providing a better platform for investigating the effects of applied voltage, or electric field strength, on resolution.

The design of IMS drift cells is complicated because the cell geometries that lead to increased resolution also decrease ion transmission, *viz.* increasing drift length and drift gas pressure results in increased ion losses due to diffusion. Furthermore, an increase in the electric field strength increases the effective temperature of the ions that could result in structural rearrangement and/or fragmentation of the ions [31]. We introduced the use of a

* Corresponding author. Tel.: +1 979 845 3345.
*E-mail addresses:* russell@chem.tamu.edu, russell@mail.chem.tamu.edu (D.H. Russell).

1387-3806/$ – see front matter. Published by Elsevier B.V.
doi:10.1016/j.ijms.2010.08.016

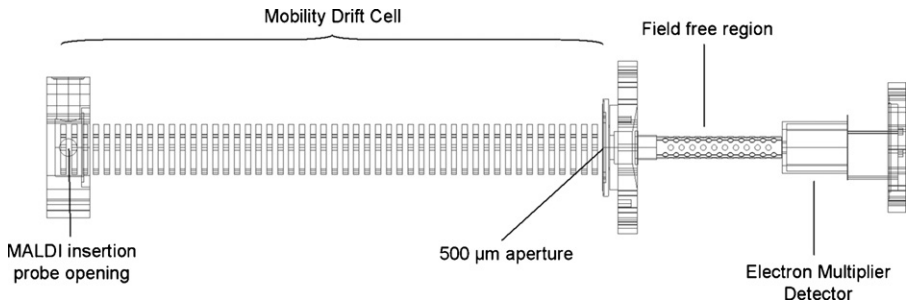


**Fig. 1.** A schematic of the MALDI-IMS instrument. The periodic-focusing DC ion guide (PDC IG) is composed of 50 electrodes with a total drift length of 63 cm. The drift length is increased to 125 cm and is composed of 100 electrodes of similar design.

PDC IG drift cell to provide increased ion transmission by means of correcting for the radial diffusion of ions [32,33]. In addition, the periodic-focusing design offers mobility separations at lower pressures (1–3 torr) where uniform field IMS suffers from low ion transmission owing to the lack of a radial-focusing mechanism. Operation of the drift cell at reduced pressure leads to faster mobility separation and allows for higher frequency ion introduction thereby increasing instrument duty cycle and sample throughput [34–36].

Here, we evaluate the performance of increased length PDC IG drift cells in terms of ion transmission and resolution. Specifically, we present two different drift cell lengths to examine ion mobility resolution as a function of voltage. Also, two different periodic-focusing drift cell electrode geometries are simulated with SIMION and tested experimentally to compare focal properties of the electrodes and their effect on ion transmission and resolution. Finally, the electrode focal properties are examined as a function of drift gas pressure to determine an optimum pressure range for maximized ion transmission and resolution.

## 2. Experimental

### 2.1. Chemicals

A fullerene mixture, $C_{60}$ (MW = 720 Da) and $C_{70}$ (MW = 840 Da), was purchased from Sigma–Aldrich (St. Louis, MO). The peptide Val-4-Angiotensin I (MW = 1208.4 Da), amino acid sequence NRVVIHPFNL, and Glu-Fibrinopeptide B (MW = 1569.6 Da) were purchased from American Peptide Company, Inc. (Sunnyvale, CA) and used without further purification. A suspension of fullerene in benzene was deposited on the stainless steel MALDI probe target and allowed to dry prior to analysis. The peptides were dissolved in distilled water at a concentration of 1 mg ml$^{-1}$ and mixed 1:1 (v:v) with 5 mg ml$^{-1}$ alpha-cyano-4-hydroxycinnamic acid in 60 percent acetonitrile, 40 percent distilled water with 0.1 percent trifluoroacetic acid solution and 10 mM dihydrogen ammonium phosphate. The mixture of peptide and matrix was then spotted on the MALDI target.

### 2.2. Instrumentation

The schematic drawing of the MALDI-IMS instrument used in these studies is contained in Fig. 1. Samples are spotted on a stainless steel probe that is inserted into the drift cell between the first and second electrode. The ions formed by MALDI (nitrogen laser, λ = 337 nm (Stanford Research Systems, Sunnyvale, CA)) drift through a 63 cm drift cell composed of 50 individual electrodes (see Section 2.3) operated at pressures between 1 and 3 torr. The electrodes are connected by 1 MΩ high-precision resistors (Mouser Electronics, Mansfield, TX) to establish a linear voltage drop across the drift cell. Ions exit the drift cell through a 500 μm aperture which provides a vacuum differential between the drift cell and the ion detector region. The aperture plate is connected to ground through a high-precision 2.88 MΩ resistor (Mouser Electronics, Mansfield, TX), and the resulting voltage drop serves to accelerate the ions toward the detector (Galileo Channeltron electron multiplier (CEM); Burle Electro-Optics, Inc.; Lancaster, PA).

Experiments were also performed on a 125 cm drift cell composed of 100 individual electrodes of similar design to that of the 63 cm drift cell. All ion mobility experiments presented herein were conducted at room temperature (~300 K), and this temperature was used to calculate the $E/N$ from the experimental value of $E/p$ [31,37]. Specific operating conditions used in obtaining individual ion mobility spectra are given in the relevant figures and captions.

### 2.3. Electrodes

The electrode dimensions (inner diameter ($d$), thickness ($t$) and spacing between the electrodes ($s$)) define the periodic-focusing drift field. Here, we examine two different electrode aspect ratios: electrode configuration A where $d$, $t$, and $s$ are 6.35 mm (aspect ratio 1:1:1) and electrode configuration B where $d$ is 8 mm while $t$ and $s$ are 6.35 mm (aspect ratio approximately 4:3:3). These two electrodes were used to estimate the effects of the electrode design on both resolution and ion transmission compared with uniform field electrodes. For the uniform field electrodes, $d$ is 50 mm and $t$ and $s$ are 6.35 mm.

### 2.4. Simulations

SIMION version 8.0 [38] (SIS, Ringoes, NJ) simulations were performed for $C_{60}^{\bullet+}$, with an ion-neutral collision cross section of 124 Å$^2$, to investigate resolution and ion transmission for different drift cell electrodes. Ion-neutral collisions were simulated using helium as the drift gas with the collision_hs1.lua user program provided with SIMION employing a hard-sphere collision model.

## 3. Results and discussion

The PDC IG was developed in our laboratory for increased ion transmission for dispersive IMS [32]. Briefly, the device consists of a series of stacked, thick electrodes that radially confine ions near the center of the drift axis, thereby increasing overall ion transmission. This design takes advantage of the nonlinear (fringing) electric fields at the edges of each electrode when an electrical potential is applied across the electrode stack. These conditions are very different from those typically employed for uniform field IMS drift cells. For example, the inner diameter of the electrodes used for uniform field drift cells is large relative to the electrode thickness, whereas the inner diameter of the PDC IG is relatively smaller and approximately equivalent to that of the electrode thickness. The geometry (diameter, thickness and spacing) of the electrodes is critical to the

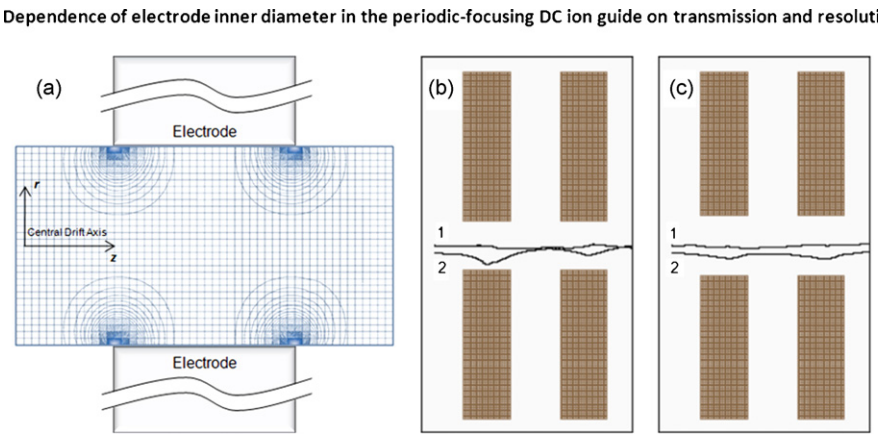


**Fig. 2.** "Effective potential" contours considering only the radial electric field variations for the 6.35 mm inner diameter drift cell (a). Cross section of two electrodes from the 6.35 mm inner diameter (b) and 8 mm inner diameter (c) drift cell showing two representative ion trajectories at 29 V cm$^{-1}$ torr$^{-1}$ ($(E/N)$ = 90 Td).

focusing properties of the device. The radial ($r$) ion confinement is observed as a slow drift of the off-axis ($r \neq 0$) ion trajectories towards the center ($r$ = 0) (Fig. 2(b), ion trajectory 2) that may be explained using "effective potentials" that extend from the edges of thick electrodes (Fig. 2(a)). Furthermore, the axial electric field and drift gas pressure determine the drift velocity of the ions which also influences the ion focusing. Clearly ions having different radial positions with respect to the electrode surface experience different magnitude effective potentials (Fig. 2(b) and (c)). As ions diffuse to increased radial positions ($r \neq 0$) they experience greater magnitude effective potentials and are refocused toward the central drift axis ($r$ = 0) upon exiting an electrode. After exiting an electrode all ions experience a relatively large potential drop and are accelerated by the electric field. We previously showed that under similar conditions the mobility separation corresponds to low-field conditions for large molecule ions, *i.e.*, peptides of the size examined in this study [31]. A more rigorous theoretical treatment of the focusing mechanism, which includes consideration of the effective ion temperature ($T_{eff}$), of the PDC IG is presented elsewhere [37].

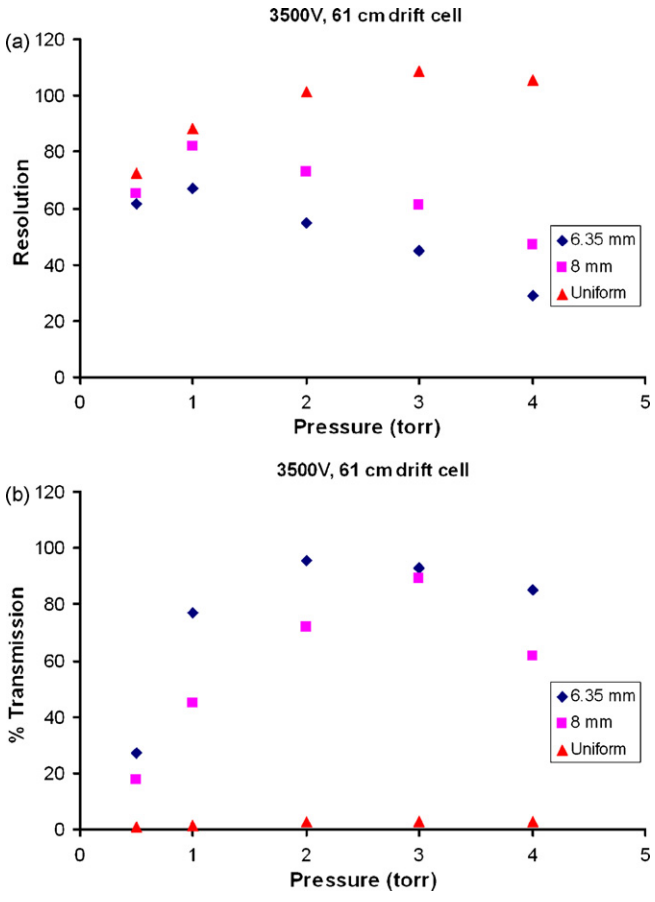


**Fig. 3.** SIMION simulation results depicting resolution (a) and percent transmission (b) as a function of pressure for two PDC IG geometries and a uniform field drift cell 61 cm in length with an applied voltage of 3500 V.

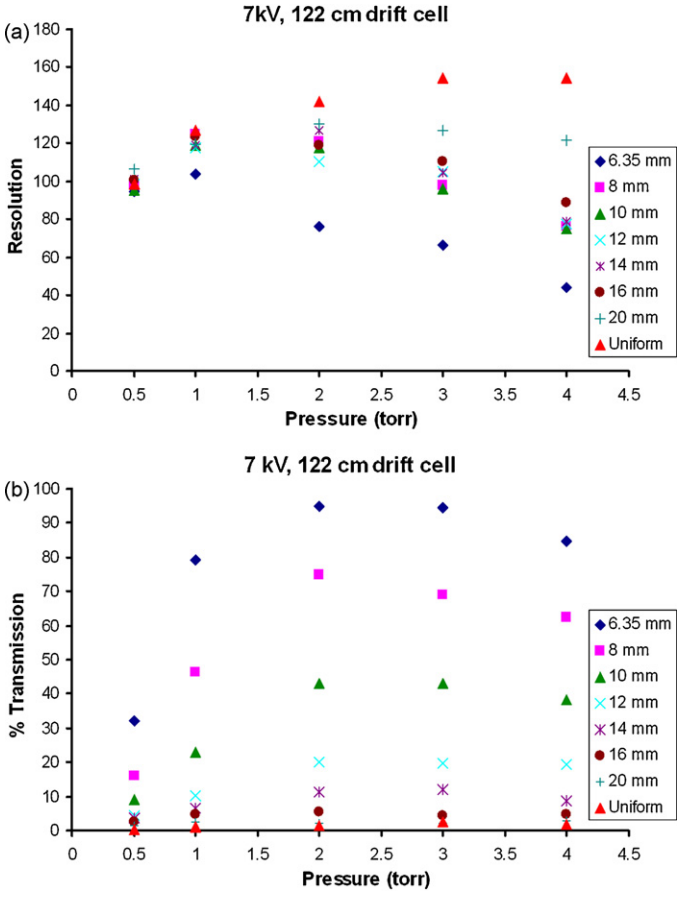


**Fig. 4.** SIMION simulation results of resolution (a) and percent ion transmission (b) versus pressure for several drift cell electrode geometries with various inner diameters denoted in the figure legend. The simulations were performed on a 122 cm drift cell with an applied voltage of 7000 V.

Fig. 3 contains theoretical plots of resolution and percent ion transmission versus pressure for the molecular ion $C_{60}^{\bullet+}$ (molecular weight = 720 Da) for three electrode geometries. These simulations were performed for a drift length of 61 cm, an applied voltage of 3500 V and a 1 mm aperture at the exit of the drift cell. The slight variation in drift length and aperture size compared to the instrumental drift length and aperture size is due to the millimeter to grid unit ratio in SIMION.

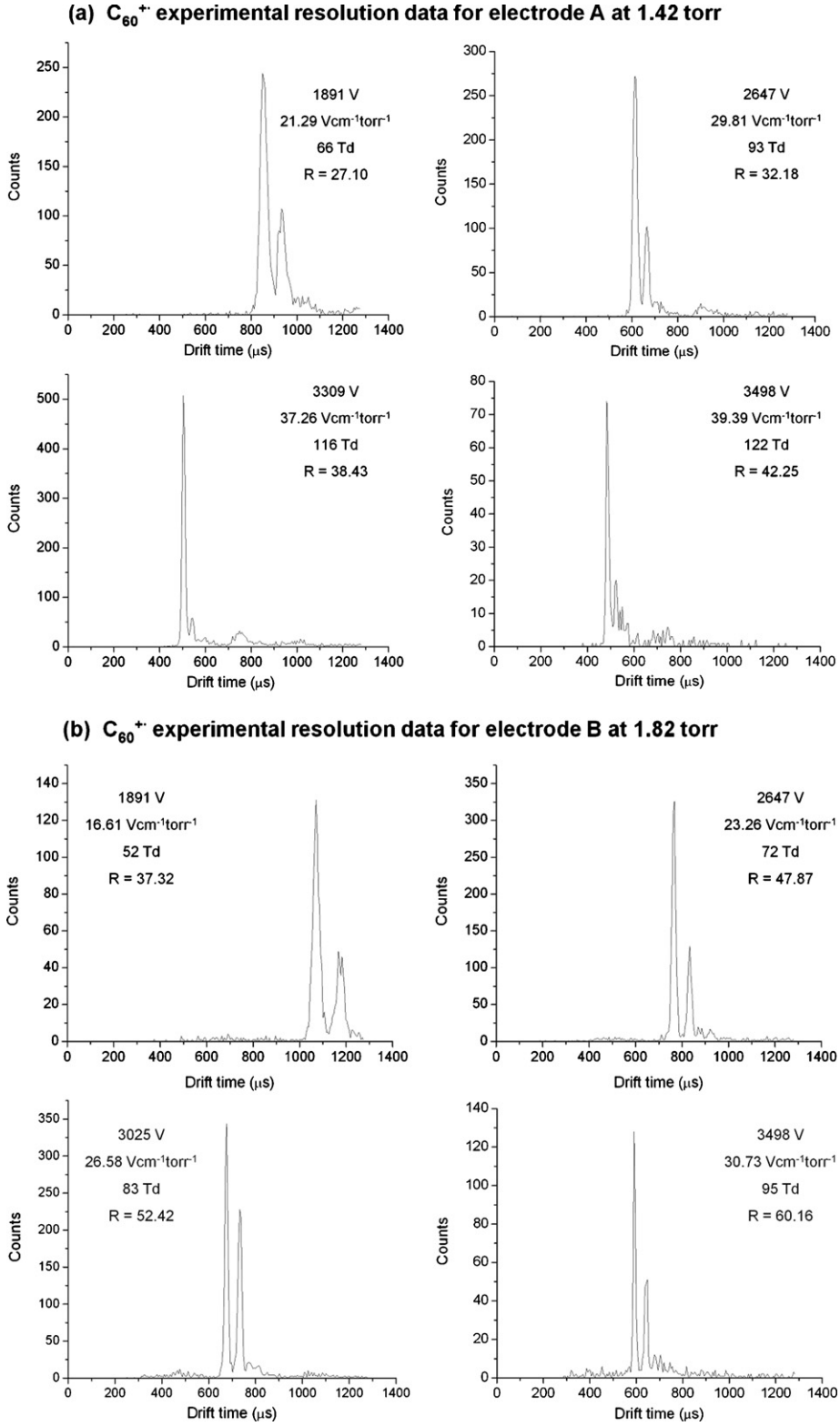


**Fig. 5.** Experimental ion mobility spectra of $C_{60}^{\bullet+}$ and $C_{70}^{\bullet+}$ obtained from a 63 cm PDC IG equipped with 6.35 mm inner diameter electrodes (electrode configuration A) (a). Experimental ion mobility spectra of $C_{60}^{\bullet+}$ and $C_{70}^{\bullet+}$ obtained from the 63 cm PDC IG equipped with 8 mm inner diameter electrodes (electrode configuration B) (b). The applied voltage, $E/p$ ($E/N$) values, and mobility resolution, $R$, are reported for $C_{60}^{\bullet+}$. The drift gas pressure for all spectra in (a) was 1.42 torr while for all spectra in (b) was 1.82 torr.

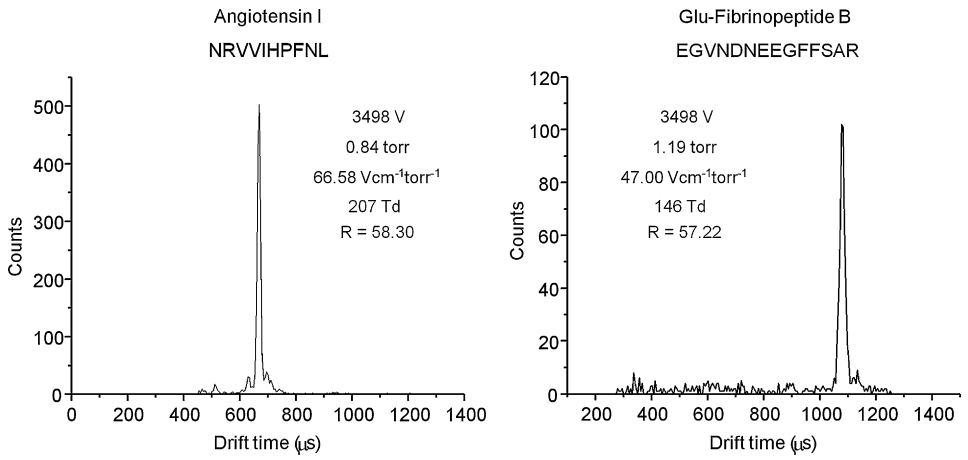


**Fig. 6.** Ion mobility spectra displaying the highest mobility resolution achieved for peptide ions on the 63 cm PDC IG equipped with 8 mm inner diameter electrodes (electrode configuration B). The applied voltage, drift gas pressure, $E/p$ ($E/N$) values, and mobility resolution, $R$, are displayed.

As illustrated by Fig. 3(a), the uniform field drift cell yielded the highest resolution but the overall ion transmission is extremely low. For example, the simulations suggest that the ion transmission is less than 3 percent for all pressures investigated for the uniform field. This value can be compared to that of electrode configuration A, which refocuses radially diffusing ions to the center of the cell, and provides a 40-fold increase in ion transmission versus uniform field electrodes. This focusing effect becomes more pronounced with decreasing inner diameter due to an increase in the effective potentials felt by an ion at an equivalent radial position [37]. This is evident from the increased ion transmission of electrode configuration A compared to electrode configuration B. On the other hand, smaller inner diameter electrodes produce a larger difference in drift length for on- and off-$z$ axis ($r \neq 0$) ion trajectories, which ultimately broadens the ion packet and degrades mobility resolution (Fig. 2(b) and (c)). This is evident by the higher resolution of electrode configuration B versus electrode configuration A (a maximum resolution increase of 22 percent over configuration A for all pressures investigated). A comparison to uniform field electrodes reveals that configuration B decreases resolution by only 10 percent at pressures of 1–2 torr. Although the larger inner diameter of configuration B leads to a slight decrease in ion transmission when compared to configuration A, the increase in ion transmission of configuration B compared to uniform field electrodes is still significant—approximately 28 times.

A second simulation investigated resolution and percent ion transmission for multiple inner diameter electrodes at various pressures on a drift cell 122 cm in length with a mobility exit aperture 1 mm and 7000 V applied across the drift cell. The first simulations contained in Fig. 3(a) suggests that an increase in electrode inner diameter increases resolution, which is confirmed by the simulations shown in Fig. 4(a). Specifically, the simulations at pressures of 3 and 4 torr reveal that mobility resolution increases as electrode inner diameter increases. The initial observation on electrode inner diameter versus percent ion transmission from Fig. 3(b) was also confirmed by Fig. 4(b). In addition, the maximum resolution for different electrode inner diameters appears to be pressure dependent while the maximum ion transmission for all the electrodes is observed between 2 and 3 torr.

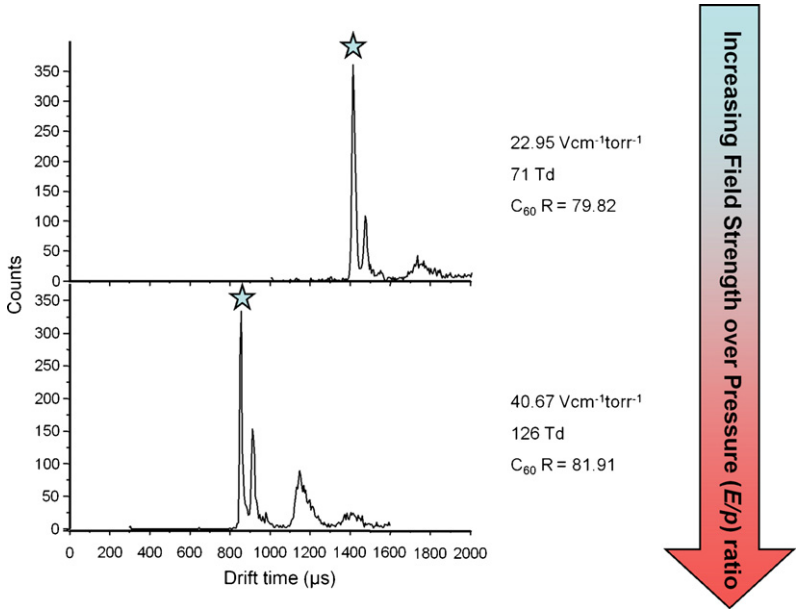


**Fig. 7.** Drift time data from a fullerene mixture taken on the 125 cm PDC IG drift cell at two different $E/p$ ($E/N$) values. The signal response for $C_{60}^{\bullet+}$ is denoted by the star while the mobility resolution is presented at right.

The two periodic-focusing electrode geometries, configuration A ($d$ = 6.35 mm) and configuration B ($d$ = 8 mm) were also tested experimentally for resolution at different pressures. Simulations suggest that the maximum resolution for configuration A and configuration B are between pressures of 1 and 2 torr with 3500 V applied across the cell. This was also confirmed experimentally in that the highest resolution measurements at approximately 3500 V were at pressures of 1.42 torr for configuration A and 1.82 torr for configuration B, respectively. Multiple field strengths are also investigated for each of the electrodes at the respective pressures to illustrate the proportionality of electric field and resolution presented in Eq. (1) (Fig. 5(a)).

The highest resolution for laser desorbed $C_{60}^{\bullet+}$ ions at 3500 V for configuration A at a pressure of 1.42 torr is 42.25 (Fig. 5(a)). At a pressure of 1.82 torr, configuration B yields a resolution of 60.16 with 3500 V across the cell (Fig. 5(b)). Notice that the simulated values (Fig. 3(a)) are also in the range of these experimental values. The maximum resolution of configuration B represents a 42 percent increase over the maximum of configuration A. Experimentally, configuration B increases resolution by an average of 20–30 percent versus configuration A with only a slight decrease in ion transmission. It should be noted that an equivalent drift length was tested with uniform field electrodes and no appreciable signal was seen after 20 min of acquisition time, as suggested by the results of low percent transmission in SIMION simulations.

Two peptides were also studied, using configuration B for the drift cell electrodes, in the 63 cm length drift cell. The peptides were Val-4-Angiotensin I peptide, with amino acid sequence NRVVIHPFNL, and Glu-Fibrinopeptide B (Fig. 6). The maximum resolution for each peptide approached 60, similar to the maximum resolution for $C_{60}^{\bullet+}$.

The pressure at which the maximum resolution was attained becomes important when considering low-field versus high-field mobility conditions. It is of utmost importance that in any mobility separation, especially for low mass ions, the contribution from the field energy to the overall ion energy and the resulting effective ion temperature, $T_{eff}$, be considered. The values of $E/p$, or $E/N$, become very important as applied voltage is increased or temperature is decreased. As $E/p$ ($E/N$) is increased, the field energy, or energy gained by the ions due to the accelerating field, can raise the effective temperature of the ion to a point where ion mobility is no longer independent of the electric field [10]. There is intrinsic value in increasing field strength for separations as sensitivity is increased and separation times are reduced [39], but $T_{eff}$ becomes critical especially if ion-neutral collision cross section data is desired [31,40,41].

However, as ion mass increases larger $E/p$ ($E/N$) values can be achieved while maintaining low effective ion temperatures. This can be demonstrated by comparing the deviations of the reduced mobility values with increasing $E/p$ ($E/N$) values. The results for reduced ion mobility versus $E/p$ ($E/N$) of the analytes studied agree well with previously published data where $C_{60}^{\bullet+}$ enters the high-field mobility limit at approximately 30–40 V cm$^{-1}$ torr$^{-1}$, evidenced by the deviation of the reduced ion mobility at this value of $E/p$ [39]. The peptides show a slight deviation in reduced mobility between 60 and 70 V cm$^{-1}$ torr$^{-1}$. Therefore, as ion mass increases the field energy can be increased to higher values without a deviation in mobility.

Another important point to note is that Eq. (1), the theoretical representation of diffusion limited resolving power, was derived for atomic ions separated with uniform field electrodes. As ion mass increases, experimental resolution never reaches the theoretical diffusion limited resolving power [42]. Factors leading to peak broadening are initial size and shape of the pulsed ion packet from a pulsed ionization source or gated continuous ion source [14,42–45], expansion of initial ion packet due to coulombic repulsion [42,46], reactions with neutral contaminants, and the presence of different ion conformations – especially for peptide and protein ions [16,21,40,47].

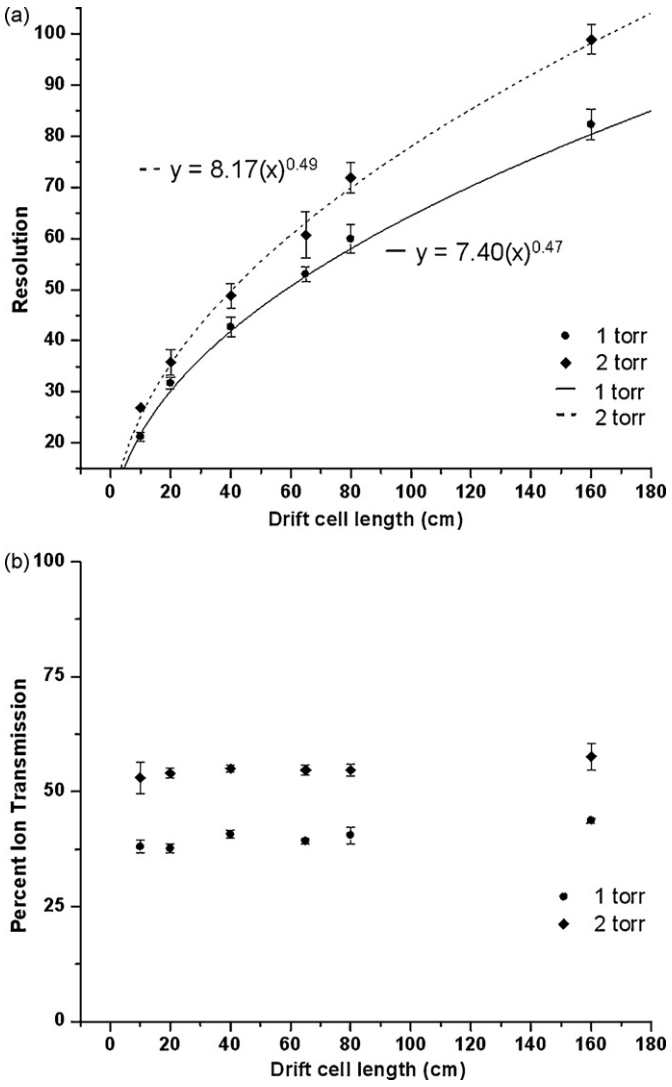


**Fig. 8.** Plot of resolution (a) and percent ion transmission (b) versus drift cell length at pressures of 1 and 2 torr for a PDC IG with 8 mm inner diameter electrodes, configuration B. The error bars were calculated for three simulation trials. The lines shown in (a) are the best-fit lines that approach a square-root dependence of the resolution on drift cell length. The equations for the lines are shown in (a).

According to simulations in Figs. 2(a) and 3(a), doubling the drift length should increase the resolution of $C_{60}^{\bullet+}$ up to 45 percent. The increase in resolution can be attributed to an increase in applied voltage that is possible through the increased drift length while maintaining a low $E/p$ ($E/N$) value in the drift cell. The experimental data for a fullerene mixture acquired using the 125 cm PDC IG drift cell is presented in Fig. 7. The data is plotted showing mobility drift time at two different $E/p$ ($E/N$) ratios. The maximum resolution of 82 corresponds to an increase of 36 percent over that obtained using the 63 cm drift cell, which is in good agreement with the predicted increase from Eq. (1).

Additional simulations were performed in order to further investigate the dependence of resolution and ion transmission in periodic-focusing ion mobility on the applied voltage and drift cell length at pressures of 1 and 2 torr (Fig. 8). The parameters for the simulation are as follows: $C_{60}^{\bullet+}$ as the analyte, 8 mm inner diameter electrodes (configuration B), 1 mm inner diameter exit aperture, He drift gas, an $E/p$ value of 30 V cm$^{-1}$ torr$^{-1}$ (($E/N$) = 93 Td) for all

drift lengths (so that the voltage scales with the drift length). The data in Fig. 8(a) illustrates that, as expected from Eq. (1), the resolution increase is proportional to the square root of the drift cell length. For a drift length of 65 cm the mobility resolution is 53 and 61 at 1 and 2 torr, respectively. The results from the simulation are in good agreement with a resolution of 60 from the experimental data for the 63 cm drift cell. Likewise, for a drift length of 125 cm the simulated resolution is approximately 70–85 between 1 and 2 torr, while experiments yielded a resolution of 82.

The results for percent ion transmission are of utmost importance and need to be emphasized to explain the major analytical utility of the PDC IG. Fig. 8(b) shows that percent ion transmission remains constant, approximately 40 percent at 1 torr and 55 percent at 2 torr, regardless of drift cell length. For a uniform field drift cell, ion transmission decreases exponentially with drift cell length. Herein lies the main advantage of periodic-focusing in that ion transmission is independent of drift cell length; rather, ion transmission is dependent on electrode geometry, applied electric field, and aperture size used at the mobility exit. It can be estimated that ion transmission with the same parameters and a 500 μm aperture is approximately 10–15 percent in the pressure range of 1 and 2 torr. Ion transmission in a PDC IG would increase by increasing the aperture size or the applied electric field.

## 4. Conclusion

An investigation of the effect of drift length, applied voltage and electrode geometry on the performance of periodic-focusing DC ion guide (PDC IG) drift cells demonstrates increased ion transmission without a significant decrease in resolution when compared to uniform electric field configurations. Results from SIMION trajectory simulations suggests that an optimally designed drift cell operating at pressures of 1–2 torr can achieve ion transmission of 30–40 percent with a small decrease (10 percent) in resolution relative to that of a uniform electric field.

Experimental data for a 63 cm PDC IG composed of electrode configuration B, yielded a maximum resolution of 60 for the radical cation of $C_{60}$ and the $[M+H]^+$ ions of two model peptides. Increasing the drift length ($L$) by a factor of two (125 cm drift cell), which allows higher voltages ($EL$) to be applied across the drift cell, increases the resolution obtained to ~82, a 36 percent increase compared to the 63 cm drift cell. Eq. (1) reveals that $R$ should scale as $L^{1/2}$, corresponding to a 41 percent increase in $R$, which is in good agreement with the observed increase.

Finally, it is interesting to project the practical significance of the manipulation of the variables contained from Eq. (1) in the limit of an ion population composed of a single conformer. For example, an increase in drift length ($L$) to 250 cm should provide an additional 41 percent increase in $R$, and increasing the field strength ($E$) of a 250 cm drift cell by a factor of 4 could potentially provide a 100 percent increase in resolution. In addition, operation of the drift cell at reduced temperature ($T$), *i.e.*, 100 K rather than ambient (300 K), could provide an additional 70 percent increase in $R$ [28]. Thus, optimization of the drift cell design and operational parameters in terms of $L$, $E$, and $T$ could potentially increase mobility resolution to ~400 for a singly charged ion!

## Acknowledgements

The authors would like to thank Greg Matthijetz for his expertise in electronics, Will Seward and Carl Johnson for expert machining of parts needed for the instrument and Al Schultz and Tom Egan of Ionwerks, Inc. (Houston, TX) for the data acquisition system used in this work. The National Science Foundation—Major Research Instrumentation Program DBI-0821700 and the Department of Energy, Division of Chemical Sciences, BES DE-FG02-04ER15520, supported this work.

## References

[1] C. Becker, K. Qian, D.H. Russell, Molecular weight distributions of asphaltenes and deasphaltened oils studied by laser desorption ionization and ion mobility mass spectrometry, Anal. Chem. 80 (2008) 8592–8597.
[2] F.A. Fernandez-Lima, C. Becker, A.M. McKenna, R.P. Rodgers, A.G. Marshall, D.H. Russell, Petroleum crude oil characterization by IMS-MS and FTICR MS, Anal. Chem. 81 (2009) 9941–9947.
[3] B.C. Bohrer, S.I. Merenbloom, S.L. Koeniger, A.E. Hilderbrand, D.E. Clemmer, Biomolecule analysis by ion mobility spectrometry, Annu. Rev. Anal. Chem. 1 (2008).
[4] F.A. Fernandez-Lima, R.C. Blase, D.H. Russell, A study of ion-neutral collision cross-section values for low charge states of peptides, proteins, and peptide/protein complexes, Int. J. Mass Spectrom. (2009).
[5] B.T. Ruotolo, K.J. Gillig, E.G. Stone, D.H. Russell, Peak capacity of ion mobility mass spectrometry: separation of peptides in helium buffer gas, J. Chromatogr. B 782 (2002) 385–392.
[6] B.T. Ruotolo, J.A. McLean, K.J. Gillig, D.H. Russell, Peak capacity of ion mobility mass spectrometry: the utility of varying drift gas polarizability for the separation of tryptic peptides, J. Mass Spectrom. 39 (2004) 361–367.
[7] J.A. McLean, B.T. Ruotolo, K.J. Gillig, D.H. Russell, Ion mobility-mass spectrometry: a new paradigm for proteomics, Int. J. Mass Spectrom. 240 (2005) 301–315.
[8] A. Woods, M. Ugarov, T. Egan, J. Koomen, K.J. Gillig, K. Fuhrer, M. Gonin, J.A. Schultz, Lipid/peptide/nucleotide separation with MALDI-ion mobility-TOF MS, Anal. Chem. 76 (2004) 2187–2195.
[9] G.A. Eiceman, Z. Karpas, Ion Mobility Spectrometry, CRC Press, Boca Raton, 1994.
[10] E.A. Mason, E.W. McDaniel, Transport Properties of Ions in Gases, John Wiley & Sons, New York, 1988.
[11] L. Tao, J.R. McLean, J.A. McLean, D.H. Russell, A collision cross-section database of singly-charged peptide ions, J. Am. Soc. Mass Spectrom. 18 (2007) 1232–1238.
[12] H.A. Sawyer, J.T. Marini, E.G. Stone, B.T. Ruotolo, K.J. Gillig, D.H. Russell, The structure of gas-phase bradykinin fragment 1-5 (RPPGF) ions: an ion mobility spectrometry and H/D exchange ion-molecule reaction chemistry study, J. Am. Soc. Mass Spectrom. 16 (2005) 893–905.
[13] J.A. McLean, The mass-mobility correlation redux: the conformational landscape of anhydrous biomolecules, J. Am. Soc. Mass Spectrom. 20 (2009) 1775–1781.
[14] S. Rokushika, H. Hiroyuki, M.A. Baim, H.H. Hill Jr., Resolution measurement for ion mobility spectrometry, Anal. Chem. 57 (1985) 1902–1907.
[15] H.E. Revercomb, E.A. Mason, Theory of plasma chromatography/gaseous electrophoresis—a review, Anal. Chem. 47 (1975) 970–983.
[16] P. Dugourd, R.R. Hudgins, D.E. Clemmer, M.F. Jarrold, High-resolution ion mobility measurements, Rev. Sci. Instrum. 68 (1997) 1122–1129.
[17] R.R. Hudgins, J. Woenckhaus, M.F. Jarrold, High resolution ion mobility measurements for gas phase proteins: correlation between solution phase and gas phase conformations, Int. J. Mass Spectrom. Ion Process. 165/166 (1997) 497–507.
[18] P.R. Kemper, N.F. Dupuis, M.T. Bowers, A new, higher resolution, ion mobility mass spectrometer, Int. J. Mass Spectrom. 287 (2009) 46–57.
[19] R. Kurulugama, F.M. Nachtigall, S. Lee, S.J. Valentine, D.E. Clemmer, Overtone mobility spectrometry. Part 1. Experimental observations, J. Am. Soc. Mass Spectrom. 20 (2009) 729–737.
[20] S.I. Merenbloom, R.S. Glaskin, Z.B. Henson, D.E. Clemmer, High-resolution ion cyclotron mobility spectrometry, Anal. Chem. 81 (2009) 1482–1487.
[21] A.A. Shvartsburg, R.R. Hudgins, P. Dugourd, M.F. Jarrold, Structural elucidation of fullerene dimers by high-resolution ion mobility measurements and trajectory calculation simulations, J. Phys. Chem. A 101 (1997) 1684–1688.
[22] S.J. Valentine, S.T. Stokes, R. Kurulugama, F.M. Nachtigall, D.E. Clemmer, Overtone mobility spectrometry. Part 2. Theoretical considerations of resolving power, J. Am. Soc. Mass Spectrom. 20 (2009) 738–750.
[23] J.G. Slaton, H.A. Sawyer, D.H. Russell, Low-pressure ion mobility-time-of-flight mass spectrometry for metalated peptide ion structural characterization: tyrosine-containing tripeptides and homologous septapeptides, Int. J. Ion Mobil. Spectrom. 8 (2005) 13–18.
[24] C.A. Srebalus, J. Li, W.S. Marshall, D.E. Clemmer, Gas-phase separations of electrosprayed peptide libraries, Anal. Chem. 71 (1999) 3918–3927.
[25] C. Wu, W.F. Siems, G.R. Asbury, H.H. Hill Jr., Electrospray ionization high-resolution ion mobility spectrometry-mass spectrometry, Anal. Chem. 70 (1998) 4929–4938.
[26] C. Wu, W.F. Siems, J. Klasmeier, H.H. Hill Jr., Separation of isomeric peptides using electrospray ionization/high-resolution ion mobility spectrometry, Anal. Chem. 72 (2000) 391–395.
[27] M. Zhu, B. Bendiak, B. Clowers, H.H Hill Jr., Ion mobility-mass spectrometry analysis of isomeric carbohydrate precursor ions, Anal. Bioanal Chem. 394 (2009) 1853–1867.
[28] J.C. May, Development of a cryogenic drift cell spectrometer and methods for improving the analytical figures of merit for ion mobility-mass spectrometry analysis, Ph.D. Dissertation, Department of Chemistry, Texas A&M University, 2009.

[29] M. Tabrizchi, Temperature effects on resolution in ion mobility spectrometry, Talanta 62 (2004) 65–70.
[30] G.F. Verbeck, K.J. Gillig, D.H. Russell, Variable-temperature ion mobility time-of-flight mass spectrometry studies of electronic isomers of $Kr^{2+}$ and $CH_3OH^{+\bullet}$ radical cations, Eur. J. Mass Spectrom. 9 (2003) 579–587.
[31] F.A. Fernandez-Lima, H. Wei, Y.Q. Gao, D.H. Russell, On the structure elucidation using ion mobility spectrometry and molecular dynamics, J. Phys. Chem. A 113 (2009) 8221–8234.
[32] K.J. Gillig, B.T. Ruotolo, E.G. Stone, D.H. Russell, An electrostatic focusing ion guide for ion mobility-mass spectrometry, Int. J. Mass Spectrom. 239 (2004) 43–49.
[33] K.J. Gillig, D.H. Russell, Periodic field focusing ion mobility spectrometer, US Patent 6,639,213 B2, 2003.
[34] W. Sun, J.C. May, K.J. Gillig, D.H. Russell, A dual time-of-flight apparatus for an ion mobility-surface-induced-dissociation-mass spectrometer for high-throughput peptide sequencing, Int. J. Mass Spectrom. 287 (2009) 39–45.
[35] J.A. McLean, W.K. Russell, D.H. Russell, A high repetition rate (1 kHz) microcrystal laser for high throughput atmospheric pressure MALDI-quadrupole-time-of-flight mass spectrometry, Anal. Chem. 75 (2003) 648–654.
[36] J.A. McLean, D.H. Russell, Data acquisition based on analyte dispersion in two dimensions: more signal more of the time, Int. J. Ion Mobil. Spectrom. 8 (2005) 66–71.
[37] J.A. Silveira, C.M. Gamage, R.C. Blase, J.C. May, D.H. Russell, Gas-phase ion dynamics in a periodic-focusing dc ion guide, Int. J. Mass Spectrom. (2010), in press, doi:10.1016/j.ijms.2010.07.019.
[38] *SIMION*, version 8.0; Scientific Instrument Services, Inc., Ringoes, NJ, 2006.
[39] B.T. Ruotolo, J.A. McLean, K.J. Gillig, D.H. Russell, The influence and utility of varying field strength for the separation of tryptic peptides by ion mobility-mass spectrometry, J. Am. Soc. Mass Spectrom. 16 (2005) 158–165.
[40] P.R. Kemper, M.T. Bowers, Electronic-state chromatography: application to first-row transition-metal ions, J. Phys. Chem. 95 (1991) 5134–5146.
[41] L.A. Viehland, E.A. Mason, Gaseous ion mobility in electric fields of arbitrary strength, Ann. Phys. 91 (1975) 499–533.
[42] P. Watts, A. Wilders, On the resolution obtainable in practical ion mobility systems, Int. J. Mass Spectrom. Ion Process. 112 (1992) 179–190.
[43] G.R. Asbury, H.H. Hill Jr., Evaluation of ultrahigh resolution ion mobility spectrometry as an analytical separation device in chromatographic terms, J. Microcolumn Sep. 12 (2000) 172–178.
[44] A.B. Kanu, M.M. Gribb, H.H. Hill Jr., Predicting optimal resolving power for ambient pressure ion mobility spectrometry, Anal. Chem. 80 (2008) 6610–6619.
[45] W.F. Siems, C. Wu, E.E. Traver, H.H. Hill Jr., Measuring the resolving power of ion mobility spectrometers, Anal. Chem. 66 (1994) 4195–4201.
[46] J. Xu, W.B. Whitten, J.M. Ramsey, Space charge effects on resolution in a miniature ion mobility spectrometer, Anal. Chem. 72 (2000) 5787–5791.
[47] S.L. Koeniger, S.I. Merenbloom, D.E. Clemmer, Evidence for many resolvable structures within conformation types of electrosprayed ubiquitin ions, J. Phys. Chem. B 110 (2006) 7017–7021.